Acta Crystallographica Section B
Structural Science
ISSN 0108-7681

Chemical bonding in energetic materials: β-NTO

Elizabeth A. Zhurova and A. Alan Pinkerton*

Department of Chemistry, University of Toledo, Toledo, OH 43606, USA

Correspondence e-mail: apinker@uoft02.utoledo.edu

Received 6 July 2000
Accepted 11 December 2000

The electron density and related properties of the quasi-stable β form of 5-nitro-2,4-dihydro-3*H*-1,2,4-triazol-3-one (NTO; space group $P2_1/c$) have been determined from a low-temperature [100 (1) K] X-ray diffraction experiment. Intensities were measured with a 2K CCD Bruker diffractometer using Ag $K\alpha$ radiation. Two detector settings, several φ settings, 0.3° ω scans and 160 s exposure time per frame gave $R_{\rm int}$ = 0.0215 for 68 989 (4080 unique) reflections and $(\sin\theta/\lambda)_{\rm max}$ = 1.23 Å^{-1}. The Hansen–Coppens [*Acta Cryst.* (1978), A**34**, 909–921] multipole model as implemented in the *XD* program gave R = 0.0333 (all reflections), which allowed calculation of the electron density, Laplacian and electrostatic potential distributions. The bonding (3,−1) critical points and the molecular dipole moment of 3.2 (1) D were also obtained. Chemical bonding in the molecule is discussed.

1. Introduction

5-Nitro-2,4-dihydro-3*H*-1,2,4-triazol-3-one (NTO) is an explosive compound that was developed at Los Alamos in 1983 as a result of an on-going explosives synthesis program (Lee & Coburn, 1988). It has been studied as a component to replace RDX (1,3,5-trinitro-1,3,5-triazacyclohexane) in bomb fill and as a replacement for sodium azide for auto airbag systems (Lee & Gilardi, 1993, and references therein). The impact sensitivity of NTO is not very high (h_{50} = 291 cm;[1] Storm *et al.*, 1990), so it is possible to crystallize this compound and perform the X-ray diffraction experiment with no danger.

NTO can be crystallized in two forms, α and β. The α form was reported as the stable one (Lee & Gilardi, 1993), however, the crystal structure (probably twinned) has not been determined, to the best of our knowledge. The β form of NTO was reported to be unstable (Lee & Gilardi, 1993) with a monoclinic unit cell (space group $P2_1/c$). It can be crystallized, for example, by cooling a hot saturated aqueous solution. The resulting ratio of α:β phases of the crystals obtained is approximately 98:2. For the β form, the unit cell contains four NTO molecules (Lee & Gilardi, 1993), each of which forms four hydrogen bonds of two types: H···O and H···N (Fig. 1*a*). The hydrogen-bonding scheme is helical in nature, following the 2_1 screw axes. Each hydrogen bond lies parallel to the *ab* plane, thus the molecules form puckered hydrogen-bonded sheets also parallel to *ab* (Fig. 1*b*). The NTO molecule (Fig. 2) is practically planar with the largest out-of-plane deviation (0.11 Å) for the O(5*a*) atom.

[1] The shorter the impact drop height, h_{50}, the greater the sensitivity. For example, quite sensitive RDX and HMX have h_{50} values of 24 and 26 cm, respectively, although insensitive TATB has h_{50} = 490 cm (Storm *et al.*, 1990).

The electron density distribution and related properties of NTO are of current interest since some empirical relationships between impact sensitivities and electrostatic potentials of energetic molecules calculated from theory were obtained by

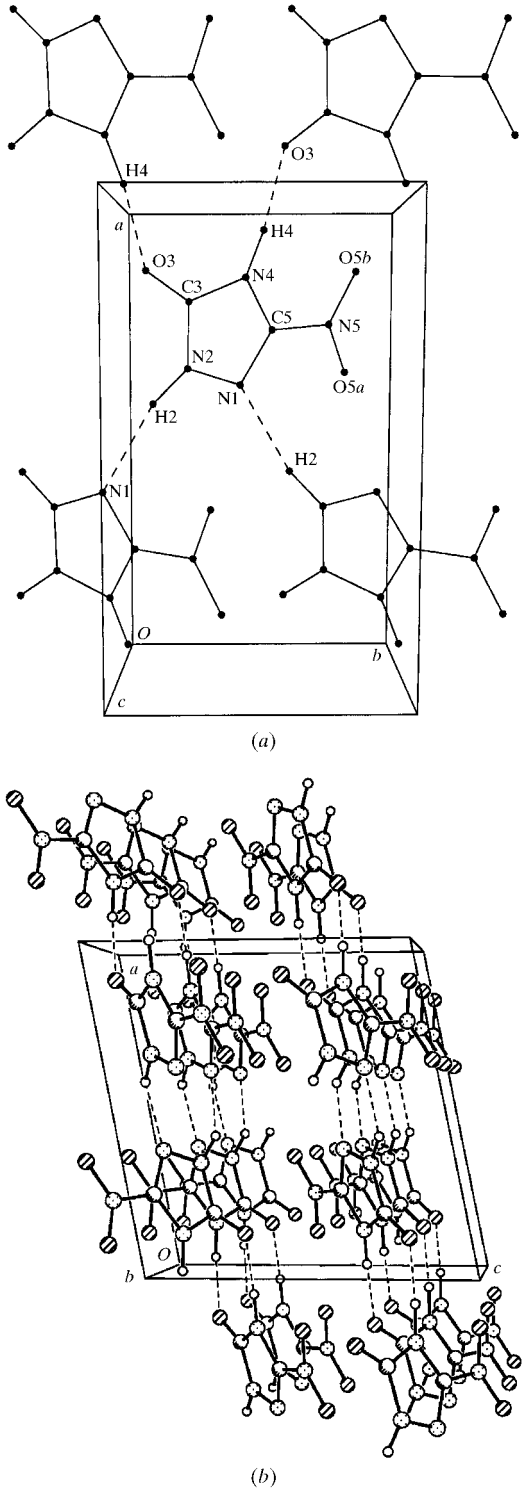

Figure 1
(*a*) Hydrogen bonds with respect to one molecule in β-NTO. (*b*) Hydrogen-bonding scheme for β-NTO showing the layer structure parallel to *ab*. The large open circles are C atoms, the dotted circles are N atoms, the striped circles are O atoms and the small open circles are H atoms.

Table 1
Experimental details.

Crystal data	
Chemical formula	$C_2H_2N_4O_3$
Chemical formula weight	130.08
Cell setting, space group	Monoclinic, $P2_1/c$
a, b, c (Å)	9.3255 (1), 5.4503 (1), 9.0400 (1)
β	101.474 (1)
V (Å^3)	450.291
Z	4
D_x (Mg m^{-3})	1.919
Radiation type	Ag $K\alpha$
Wavelength (Å)	0.56085
No. of reflections for cell parameters	8330
θ range (°)	0–27
μ (mm^{-1})	0.104
Temperature (K)	100 (1)
Crystal form, color	Plate, colorless
Crystal size (mm)	0.40 × 0.12 × 0.12
Data collection	
Diffractometer	Bruker platform
Data collection method	ω scans
No. of measured, independent and observed parameters	68 989, 6909, 4080
Criterion for observed reflections	$I > 2\sigma$ for $\sin\theta/\lambda < 1.0$, $I > 6\sigma$ for $\sin\theta/\lambda > 1.0$
R_{int}	0.0215
θ_{max} (°)	43.69
Range of h, k, l	$-22 \rightarrow h \rightarrow 22$ $-13 \rightarrow k \rightarrow 13$ $-22 \rightarrow l \rightarrow 22$
Refinement	
Refinement on	F
R, wR, S	0.0333, 0.0425, 1.132
No. of reflections and parameters used in refinement	4080, 308
H-atom treatment	All H-atom parameters refined
Weighting scheme	$w = 1/[\sigma^2(F) + 0.0001F^2]$
$(\Delta/\sigma)_{max}$	0.0000
$\Delta\rho_{max}$, $\Delta\rho_{min}$ (e Å^{-3})	0.1, −0.3
Extinction method	Isotropic Becker–Coppens (1974), type 1
Extinction coefficient	0.2195

Computer programs used: *SMART* 5.054 (Siemens, 1996*a*), *SAINT* 7.08 (Siemens, 1996*b*), *SHELXTL* (Sheldrick 1997), *XD* (Koritsanszky *et al.*, 1995).

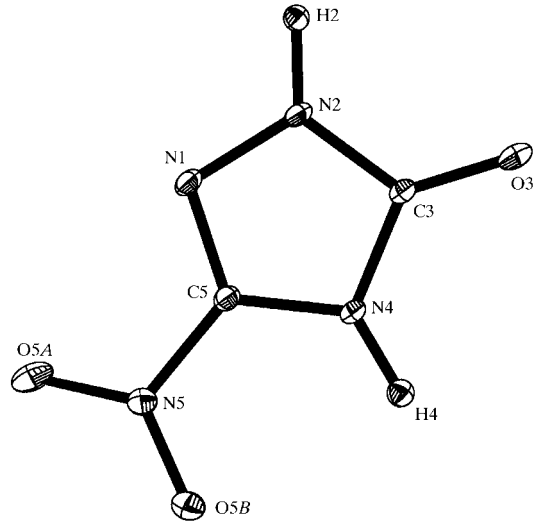

Figure 2
The NTO molecule showing 50% probability thermal ellipsoids.

Table 2
β-NTO: the results of κ refinement.

	N(2)	H(2)	O(3)	N(1)	N(4)	H(4)	C(3)	O(5*b*)	O(5*a*)	N(5)	C(5)
q, e	−0.20 (4)	+0.23 (2)	−0.48 (5)	−0.06 (4)	−0.35 (5)	+0.30 (2)	+0.37 (6)	−0.14 (4)	−0.19 (4)	+0.32 (6)	+0.21 (7)
κ'	1.006 (5)	1.22 (3)†	0.981 (4)	1.013 (5)	1.004 (5)	1.22 (3)	1.058 (9)	1.005 (4)	1.002 (4)	1.034 (6)	1.048 (9)

† The same κ set was used for both H atoms.

Murray *et al.* (1995). They found that the electrostatic potential on the molecular surface [surface with the electron density $\rho(r) = 0.001$ a.u.] of all the nitroheterocyclic molecules in their study contained maxima near the C—NO_2 bond. The electrostatic potential distribution of NTO in the plane 1.8 Å above the molecular plane was also calculated theoretically by Ritchie (1989). He obtained the electrostatic potential maximum exactly above the C(5)—N(5) bond.

In this paper we present the results from an X-ray diffraction experiment on β-NTO. The refined multipole model for the electron density allowed an additional analysis of the chemical bonding in the NTO molecule in terms of Bader's (1990) topological theory. We have calculated the electron density, Laplacian and electrostatic potential distributions for β-NTO. The characteristics of bond (3,−1) critical points were also obtained and are discussed.

2. Experimental

A transparent, colorless single crystal of the β phase of NTO was mounted on a 0.1 mm capillary with epoxy resin and slowly cooled down to 100 K with an Oxford Cryostream. The X-ray diffraction experiment was performed with a Bruker platform diffractometer with a 2K CCD detector using Ag $K\alpha$ radiation. The complete experimental protocol has been deposited.[2] 0.3° ω scans were performed at a detector distance of 3.44 cm. The exposure time of 160 s allowed the use of the full dynamic range of the detector. No intensity decay was observed during the experiment, so the crystal was considered to be stable for at least 2 weeks. Other experimental details are given in Table 1.

The integration was performed with the program *SAINT* (Siemens, 1996*b*). An empirically chosen integration box size of 1.69 × 1.82 × 0.864° and the profile fitting procedure based on strong ($I > 30\sigma$) reflections allowed us to obtain the best internal consistency ($R_{int} = 0.0215$) and preliminary refinement R factors. After the integration process, the unit-cell parameters were refined with all reflections with $\sin\theta/\lambda < 0.8$ Å^{-1}, since all the high-angle reflections were relatively weak. The integration process was repeated three times until total convergence in the cell parameters was obtained. Since the crystal size was relatively large (Table 1), the program *SADABS* (Sheldrick, 1996) was used to correct the data for the possible inhomogeneity of the X-ray beam. No absorption correction was applied ($\mu = 0.1$ mm^{-1}).

3. Refinements and results

The crystal structure was resolved and a preliminary refinement carried out with the *SHELXTL* program suite (Sheldrick, 1997). Then, the Hansen–Coppens (1978) multipole model as implemented in the *XD* program (Koritsanszky *et al.*, 1995) was used in further refinements. In this model the electron density is approximated as a sum of pseudo-atomic electron densities in the form

$$\rho_{\rm atomic}(\mathbf{r}) = \rho_{\rm core}(r) + P_v\kappa'^3\rho_{\rm valence}(\kappa' r) + \sum_{l=1}^{4}\kappa''^3 R_l(\kappa'' r)\sum_{m=-l}^{l} P_{lm}\, y_{lm}(\mathbf{r}/r).$$

The optimized parameters are a scale factor, the atomic valence-shell contraction–expansion parameters κ' and κ'', and the multipole populations P_v and P_{lm}. The refinement was carried out in two steps:

Step A: a so-called κ refinement (Coppens *et al.*, 1979) was performed. First, the scale factor, extinction, valence monopole population P_v, positional and displacement parameters were refined with the whole data set. Second, the positional and displacement parameters for non-H atoms were refined with high-angle reflections ($\sin\theta/\lambda > 0.7$ Å^{-1}) and fixed. Third, P_v, κ' parameters and extinction were refined with low-angle reflections ($\sin\theta/\lambda < 1.0$ Å^{-1}). Then, after scale factor refinement with all reflections, the procedure was repeated until the total convergence of the refined parameters. Results from this refinement are summarized in Table 2.

Step B: After that, P_v and κ' were fixed[3] and multipole parameters P_{lm} and κ'' were refined alternately with scale, positional and displacement parameters as described above.

For H atoms, all the parameters including positional and displacement ones were refined using 451 reflections with $\sin\theta/\lambda < 0.5$ Å^{-1}. Then, the N—H bond lengths were extended and fixed to the tabulated neutron values (Allen *et al.*, 1987). For the heavy atoms the multipole refinement was performed up to the hexadecapole level ($l_{max} = 4$), for H atoms only dipole populations were refined. The molecule electroneutrality condition was imposed during the refinement. In the final cycles, parameters with values less than one standard uncertainty were fixed at zero. Different κ sets were used for each of the atoms, except the H atoms. The same κ' and κ'' values were applied for both H atoms. For the initial approximation of κ' [H(2), H(4)] a value of 1.2 was taken. Isotropic secondary extinction (Table 1) was described

[2] Supplementary data for this paper are available from the IUCr electronic archives (Reference: BR0102). Services for accessing these data are described at the back of the journal.

[3] It was shown by Abramov *et al.* (1999) that to avoid *basis set overlap errors* in the evaluation of static molecular properties, physical constraints in the multipole model are necessary, such as charge or κ constraints.

according to Becker & Coppens (1974). The rigid-bond test (Hirshfeld, 1976) showed that the differences of mean-square displacement amplitudes along the interatomic vectors were less than 3×10^{-4} Å^2. The largest least-squares correlation coefficient observed was 0.43. The statistical correctness of the final results was checked by the Abrahams & Keve (1971) test. The atomic displacement ellipsoids (50% probablility) are shown in Fig. 2 and the interatomic distances are included in Table 3. The multipole, kappa, positional and thermal parameters have been deposited.

The residual electron density (the difference between experimental and calculated multipole electron densities: $\delta\rho_{res} = \rho_{exp} - \rho_{mult}$) and the static model multipole deformation electron density (the difference between calculated multipole and spherical static electron densities: $\delta\rho_{mult} = \rho_{mult} - \rho_{sph}$) maps were calculated with the low-angle reflections ($\sin\theta/\lambda < 1.0$ Å^{-1}). They are presented in Figs. 3 and 4 in the plane of the molecule. The topological analysis was performed with the *XD* program (Koritsanszky *et al.*, 1995). Using the static multipole model of the electron density, the Laplacian and electrostatic potential distributions (Tsirelson & Ozerov, 1996; Tsirelson *et al.*, 2000) were calculated (Figs. 5 and 6). The bonding (3,−1) critical points which characterize the covalent and hydrogen bonding in the NTO crystal are given in Table 3. To compare with the experimental result, a theoretical calculation (6-21G** basis set with the constrained experimental geometry) for the NTO crystal was also performed (Conrad *et al.*, 2001). An additional refinement of the multipole model based on the theoretically calculated structure factors was carried out followed by a topological analysis of the electron density. The resulting bond critical points are also included in Table 3.

The dipole moment of the molecule obtained from experimental data was 3.2 (1) D.

4. Discussion

Fig. 3 presents the residual map after the multipole refinement. The largest residual is a minimum of −0.3 e Å^{-3} at the H(2) position, however, there are no peaks greater than +/−0.15 e Å^{-3} on the interatomic bonds. In particular, there is no feature more important than −0.05 e Å^{-3} on the N(1)—N(2) line (see below). Fig. 4 presents the deformation electron density ($\delta\rho_{mult}$) maps, (*a*) in the molecular plane and (*b*) perpendicular to the plane through the N(1)—N(2) bond. Every expected covalent bond is represented by well defined

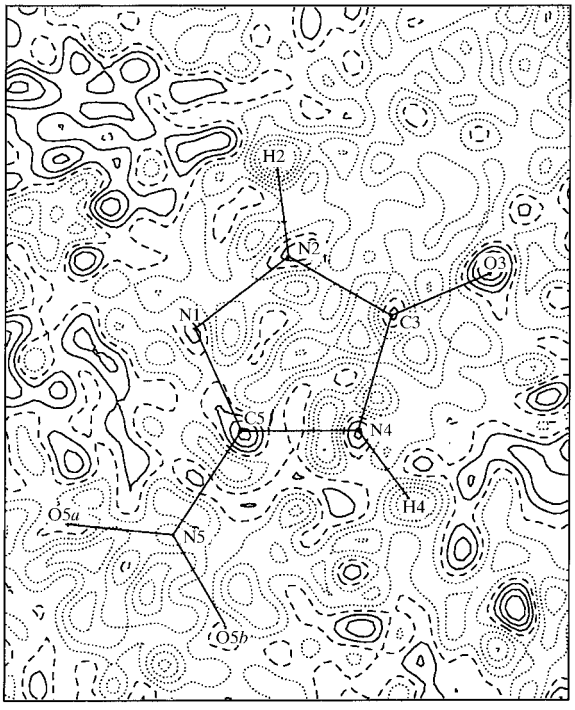

Figure 3
Difference electron density map ($\delta\rho_{res}$) in the molecular plane. Here and in Fig. 4 positive contours are solid lines, negative are dotted and the zero contour is dashed. The contour interval is 0.05 e Å^{-3}.

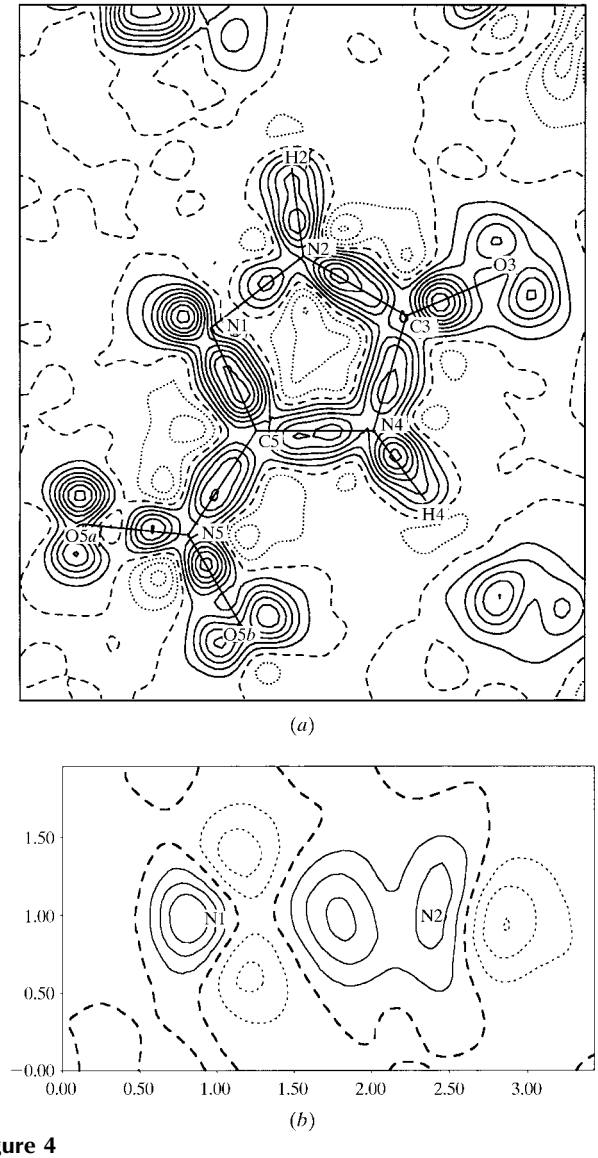

Figure 4
Deformation multipole static electron density maps ($\delta\rho_{mult}$): (*a*) molecular plane; (*b*) perpendicular section through N(1)—N(2). The contour interval is 0.1 e Å^{-3}.

Table 3
Bond critical points in β-NTO.

We report the values of the electron density (ρ, e Å^{-3}), Hessian eigenvalues (λ_1, λ_2 and λ_3) and Laplacian ($\nabla^2\rho = \lambda_1 + \lambda_2 + \lambda_3$ e Å^{-5}) at the critical point, the distances from the critical point to the first and second atoms (d_1 and d_2, Å), their sum ($d = d_1 + d_2$), internuclear distance (R, Å) and the ellipticity of the bond (ε). The first line contains the experimental results, the second line contains the theoretical calculation (6-21G** basis set) and the third one shows the results for analogous bonds in trinitrodiazapentalene (TNDP; Chen & Pinkerton, 2001).

Bond	ρ	$\nabla^2\rho$	λ_1	λ_2	λ_3	d_1	d_2	d	R	$\varepsilon = \lambda_1/\lambda_2 - 1$
N(2)—H(2)	1.98(2)	−15.34 (7)	−25.97	−23.99	34.63	0.7481	0.2611	1.0092	1.0090 (2)	0.08
	2.10 (1)	−21.41 (4)	−27.89	−26.34	32.82	0.7558	0.2532	1.0090	1.0090 (2)	0.06
N(2)—N(1)	2.30 (2)	−3.32 (7)	−19.94	−17.00	33.62	0.7016	0.6644	1.3659	1.3658 (3)	0.16
	2.21 (8)	−3.23 (7)	−18.21	−15.71	30.69	0.6921	0.6737	1.3658	1.3658 (3)	0.16
	2.41 (2)	−5.34 (4)	−21.02	−17.05	32.72	0.6858	0.6787	1.3645	1.3640 (3)	0.23
N(2)—C(3)	2.23 (3)	−20.8 (1)	−21.27	−16.94	17.45	0.7931	0.5808	1.3739	1.3737 (3)	0.26
	2.12 (2)	−15.2 (1)	−19.65	−15.08	19.55	0.7783	0.5954	1.3738	1.3737 (3)	0.30
C(3)—O(3)	2.90 (3)	−30.1 (2)	−26.43	−24.84	21.12	0.4959	0.7384	1.2343	1.2343 (3)	0.06
	2.67 (3)	−20.3 (2)	−23.62	−21.31	24.66	0.4873	0.7470	1.2343	1.2343 (3)	0.11
N(1)—C(5)	2.67 (3)	−27.5 (1)	−24.71	−19.76	16.96	0.7513	0.5476	1.2989	1.2987 (4)	0.25
	2.52 (2)	−21.9 (1)	−23.28	−16.92	18.31	0.7445	0.5542	1.2987	1.2987 (4)	0.38
	2.23 (2)	−22.14 (7)	−17.38	−13.32	8.56	0.8323	0.5562	1.3885	1.3849 (3)	0.31
N(4)—H(4)	1.93 (1)	−17.47 (4)	−26.34	−25.42	34.29	0.7704	0.2392	1.0096	1.0090 (2)	0.04
	2.03 (1)	−22.59 (3)	−28.08	−26.64	32.13	0.7740	0.2350	1.0090	1.0090 (2)	0.05
C(3)—N(4)	2.17 (2)	−17.4 (1)	−19.34	−16.07	18.00	0.5887	0.7908	1.3796	1.3795 (3)	0.21
	2.04 (2)	−14.3 (1)	−18.03	−14.34	18.08	0.5879	0.7917	1.3796	1.3795 (3)	0.26
C(5)—N(4)	2.23 (3)	−17.9 (1)	−19.60	−15.43	17.11	0.5772	0.7801	1.3573†	1.3556 (4)	0.27
	2.15 (2)	−15.91 (9)	−18.20	−14.19	16.49	0.5674	0.7887	1.3561	1.3556 (4)	0.28
N(5)—C(5)	2.01 (2)	−16.97 (9)	−18.51	−16.08	17.62	0.8033	0.6397	1.4430	1.4430 (4)	0.14
	1.89 (2)	−11.40 (7)	−16.36	−14.43	19.39	0.7803	0.6627	1.4430	1.4430 (4)	0.13
	2.24 (2)	−29.73 (8)	−19.75	−15.14	5.17	0.9007	0.5086	1.4094	1.4069 (3)	0.30
N(5)—O(5*b*)	3.39 (2)	−6.8 (1)	−33.02	−30.98	57.21	0.6022	0.6232	1.2254	1.2253 (3)	0.06
	3.17 (3)	−7.7 (1)	−29.95	−27.12	49.39	0.5807	0.6446	1.2253	1.2253 (3)	0.10
	3.44 (3)	−12.62 (9)	−31.80	−28.17	47.35	0.5755	0.6596	1.2351	1.2332 (3)	0.13
N(5)—O(5*a*)	3.27 (3)	−4.7 (1)	−31.67	−27.90	54.84	0.5976	0.6303	1.2279	1.2279 (3)	0.12
	3.12 (3)	−6.7 (1)	−29.13	−26.27	48.73	0.5832	0.6447	1.2279	1.2279 (3)	0.11
	3.33 (5)	−13.7 (1)	−32.07	−27.74	46.15	0.5820	0.6527	1.2347	1.2333 (3)	0.16
H(2)···N(1)	0.139 (2)	2.161 (1)	−0.63	−0.61	3.40	0.7614	1.2951	2.0565	2.0544 (3)	0.05
	0.125 (1)	2.397 (1)	−0.59	−0.58	3.57	0.7680	1.2953	2.0634	2.0544 (3)	0.01
H(4)···O(3)	0.290 (4)	4.057 (4)	−1.74	−1.55	7.36	0.6113	1.1129	1.7242	1.7233 (4)	0.06
	0.262 (1)	4.355 (3)	−1.52	−1.51	7.39	0.6136	1.1100	1.7236	1.7233 (4)	0.01

† Note, the critical point is significantly shifted away from the interatomic line.

$\delta\rho_{\rm mult}$ peaks. Polarization of the atoms involved in hydrogen bonding is also evident. The N(1)—N(2) bond appeared to be of particular interest. The $\delta\rho_{\rm mult}$ peak on the N(1)—N(2) line is only ∼0.25 e Å^{-3} compared with other bonds in the ring of ∼0.45–0.60 e Å^{-3}. It is also quite diffuse in the perpendicular plane (Fig. 4*b*). The interatomic distance is 1.366 (1) Å.

The Laplacian of the electron density in the molecular plane is shown in Fig. 5. It also contains the O(3) atom in the same plane from the nearest neighboring molecule. The solid contours show the negative values of the Laplacian, *i.e.* they represent the accumulation of electron density in the crystal. For the NTO molecule this accumulation is mostly around the atoms and along the chemical bonds. However, for the O atoms the electron density concentrates mainly in the non-bonding directions.

Table 3 lists all the (3,−1) critical points found in the molecule: for each bond the first line lists the experimental results, the second line contains the results after the multipole refinement based on theoretically calculated structure factors (Conrad *et al.*, 2001) and the third one contains the results for analogous bonds in trinitrodiazapentalene (TNDP; Chen & Pinkerton, 2001). For these two molecules, a semi-quantitative agreement was obtained between analogous values which were measured and calculated in the same way. The trend in the properties at the CP (critical point) is the same in each case: the electron density value at the critical point is greater

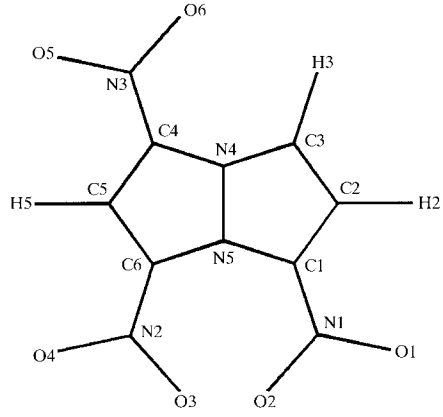

for the nitro group N(5)—O(5a,b) than for the rest of the molecule and the least negative Laplacian value is for the N(1)—N(2) bond. The ellipticities for the ring bonds are generally higher in TNDP. The positions of the critical points

indicate polarization of N—H, N—C and C—O bonds. For example, the critical point on the C(3)—O(3) bond is closer to the C(3) atom (0.4959 Å) than to O(3) (0.7384 Å), *i.e.* electrons are shifted towards oxygen. A good qualitative agreement was obtained between the experimental and theoretical results. Table 3 also lists the (3,−1) critical points associated with hydrogen bonds. The properties at the critical point on the hydrogen bonds are typical of those with similar bond lengths (see, for example, Espinosa *et al.*, 1999; Coppens *et al.*, 1999), *e.g.* the Laplacian at the critical point of the shorter [H(4)···O(3)] bond is approximately double that of the longer one [H(2)···N(1)] with greater eigenvalues in each direction.

Analysis of the chemical bonds in the triazolone ring indicates significant conjugation in all cases. N(1)—C(5) has the highest electron density value at the bond critical point and the most negative Laplacian (Table 3) and thus is the best candidate for the bond in the ring to be considered as a 'double bond'. The critical point on the C(3)—O(3) bond has even higher values for the electron density and Laplacian, so the whole picture is exactly as expected from the point of view of conventional bonding theory. The high stability of the triazolone ring was stressed by Le Campion *et al.* (1999). According to the theoretical calculations of Harris & Lammertsma (1996), the C(5)—N(5) and N—H bonds should be the first to break during chemical decomposition. In agreement with this prediction, we observe that the electron density values at the CPs on these bonds are the lowest of all bonds in the molecule. The values of ρ and $\nabla^2\rho$ at the critical point on the double C(3)—O(3) bond are in the expected range. The ellipticity of this bond is very low (0.06), however, the ellipticity of C═O bonds can vary from 0.07 to 0.14 for different types of compounds (Benabicha *et al.*, 2000).

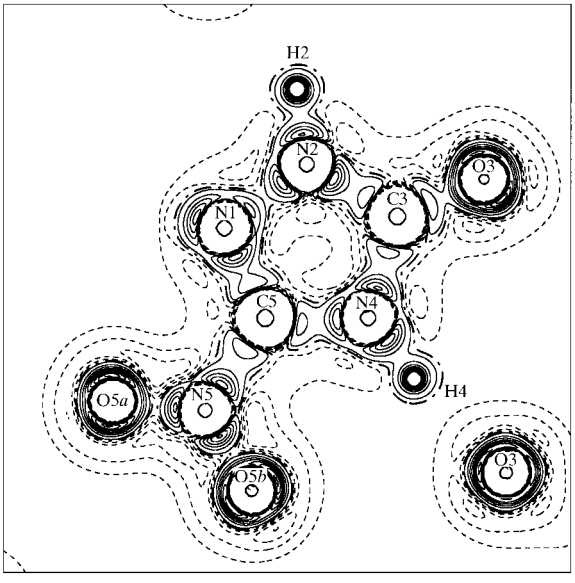

Figure 5
The Laplacian of the electron density in the molecular plane. The figure also contains the O(3) atom in the same plane from the next NTO molecule. Contours from −140 to −5 e Å^{-5} with an interval of 15 e Å^{-5} are solid lines, from 5 to 50 e Å^{-5} with an interval of 5 e Å^{-5} are dashed, the zero level is dash-dotted.

The electron density values at the critical points on the N—O bonds in NTO are relatively high: 3.39 and 3.27 e Å^{-3} (3.17 and 3.12 e Å^{-3} from the theoretical calculation), although the absolute values of the Laplacian are less compared with other bonds: −6.8 and −4.7 e Å^{-5} (−7.7 and −6.7 e Å^{-5} from theory). The topological analysis in *p*-nitroaniline (Volkov *et al.*, 2000), lithium bis(tetramethylammonium) hexanitrocobaltate(III) (Bianchi *et al.*, 1996) and *trans*-tetraaminedinitronickel(II) (Iversen *et al.*, 1997) also shows high

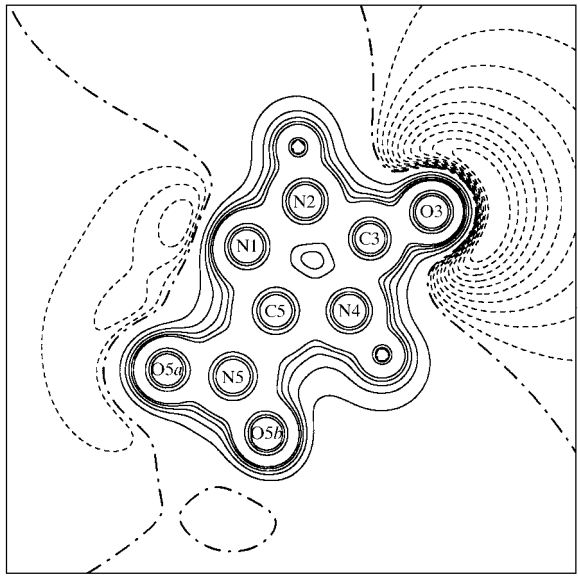

(*a*)

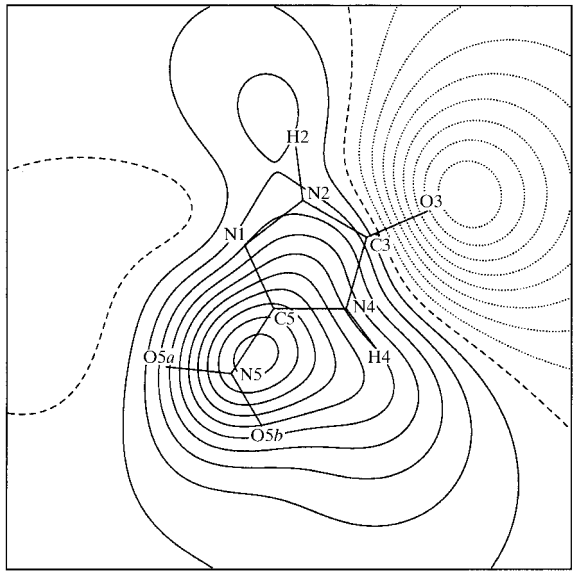

(*b*)

Figure 6
Electrostatic potential of the isolated molecule: (*a*) in the molecular plane. Contours: 0.2–1.0 e Å^{-1} with an interval of 0.2 e Å^{-1} and 4.0–8.0 e Å^{-1} with an interval of 2.0 e Å^{-1} are solid lines; −0.2 to −0.02 e Å^{-1} with interval 0.02 e Å^{-1} are dashed; the zero contour is dash-dotted. (*b*) 1.93 Å above the molecular plane. Contour interval 0.01 e Å^{-1}. Positive contours are solid lines, negative are dotted and the zero contour is dashed.

electron density values at the critical points in the N—O bonds of 3.19–3.61 e Å^{-3} and small absolute values of the Laplacian of −3.4 to −11.9 e Å^{-5}. The high electron density values on the N—O bonds can be an effect of electron donation from the oxygen lone pairs, since they are not involved in hydrogen bonding in the crystal. At the same time, the small absolute values of the Laplacian can be a result of the limited flexibility of N and O radial functions adopted in the multipole model (Bianchi *et al.*, 1996). Theoretical calculations without subsequent use of the multipole model can give similar values for the electron density, but 3–5 times greater absolute values for the Laplacian (Bianchi *et al.*, 1996; Iversen *et al.*, 1997). At the same time, a multipole refinement using theoretical structure factors leads to a better agreement with the experimental data (Howard *et al.*, 1995). Introducing separate κ parameters for different multipole orders for the N atom lowers the experimental Laplacian values from −3.4 and −3.7 e Å^{-5} to −17.8 and −18.6 e Å^{-5} (Iversen *et al.*, 1997). Finally, the observed effect on the N—O bonds can be partly due to the different locations of the critical points (the theoretical critical points are significantly shifted towards the less electronegative atom) and the significant anharmonicity of the atomic thermal motion in energetic NTO, not considered in this work.

The properties at the critical point on the N(1)—N(2) bond have similar features to the above. Although the electron density value (2.30 e Å^{-3}) is quite similar to other bonds in the ring (2.17–2.67 e Å^{-3}), the absolute value of the Laplacian is significantly less: −3.32 e Å^{-5} compared with −27.5 to −17.4 e Å^{-5}. The λ_1 and λ_2 negative Hessian eigenvalues, showing the contraction of electron density towards the bond in the perpendicular directions, are approximately the same as for all the other bonds in the triazolone ring, however, the positive λ_3 eigenvalue, showing the depletion along the bond direction, is much greater: 33.62 e Å^{-5} compared with 17.11–21.12 e Å^{-5} for the other bonds in the ring. The same feature was observed in the theoretical calculation and for the N—N bond in TNDP (Table 3). Bianchi *et al.* (1996) had found that it is λ_3 curvature which is mostly effected by the limitations of the atomic structure model described above.

The electrostatic potential distribution was also calculated using the refined multipole model. Fig. 6(*a*) shows the electrostatic potential in the molecular plane for the isolated molecule taken from the crystal. The expected negative regions around the O(3) and N(1) atoms are observed. They represent the sites of possible electrophilic attack. The electrostatic potential distribution around the nitro group is almost zero. In order to compare the result with previous theoretical predictions (Murray *et al.*, 1995; Ritchie, 1989) the electrostatic potential in the section 1.93 Å above the molecular plane was calculated (Fig. 6*b*). This distance was chosen to correspond to the electron density above the C(5)—N(5) bond of 0.0067 e Å^{-3} $\simeq$ 0.001 a.u. This electrostatic potential distribution has a maximum very close to the C(5)—N(5) bond and thus can be considered as a center for nucleophilic attack for this molecule (Murray *et al.*, 1990). Note, that C(5)—N(5) breaks first during the chemical decomposition (Harris & Lammertsma, 1996).

We appreciate the financial support of the Office of Naval Research through contract number N00014-95-1-0013. We also thank the anonymous referee for bringing our attention to the Co complexes.

References

Abrahams, S. C. & Keve, E. T. (1971). *Acta Cryst.* A**27**, 157–165.

Abramov, Yu., Volkov, A. & Coppens, P. (1999). *Chem. Phys. Lett.* **311**, 81–86.

Allen, F. H., Kennard, O., Watson, D. G., Brammer, L., Orpen, A. G. & Taylor, R. (1987). *J. Chem. Soc. Perkin Trans. 2*, pp. S1–S19.

Bader, R. F. W. (1990). *Atoms in Molecules: A Quantum Theory*. The International Series of Monographs of Chemistry, edited by J. Halpen and M. L. H. Green. Oxford: Clarendon Press.

Becker, P. J. & Coppens, P. (1974). *Acta Cryst.* A**30**, 129–147.

Benabicha, F., Pichon-Pesme, V., Jelsch, C., Lecomte, C. & Khmou, A. (2000). *Acta Cryst.* B**56**, 155–165.

Bianchi, R., Gatti, C., Adovasio, V. & Nardelli, M. (1996). *Acta Cryst.* B**52**, 471–478.

Chen, Yu.-Sh. & Pinkerton, A. A. (2001). To be published.

Conrad, H., Zhurova, E. A. & Pinkerton, A. A. (2001). To be published.

Coppens, P., Abramov, Yu., Carducci, M., Korjov, B., Novozhilova, I., Alhambra, C. & Pressprich, M. (1999). *J. Am. Chem. Soc.* **121**, 2585–2593.

Coppens, P., Guru Row, T. N., Leung, P., Stevens, E. D., Becker, P. J. & Yang, Y. W. (1979). *Acta Cryst.* A**35**, 63–72.

Espinosa, E., Souhassou, M., Lachekar, H. & Lecomte, C. (1999). *Acta Cryst.* B**55**, 563–572.

Hansen, N. & Coppens, P. (1978). *Acta Cryst.* A**34**, 909–921.

Harris, N. J. & Lammertsma, K. (1996). *J. Am. Chem. Soc.* **118**, 8048–8055.

Hirshfeld, F. L. (1976). *Acta Cryst.* A**32**, 239–244.

Howard, S. T., Hursthouse, M. B., Lehmann, C. W. & Poyner, E. A. (1995). *Acta Cryst.* B**51**, 328–337.

Iversen, B. B., Larsen, F. K., Figgis, B. N. & Reynolds, P. A. (1997). *J. Chem. Soc. Dalton Trans.* pp. 2227–2240.

Koritsanszky, T., Howard, S., Mallison, P. R., Su, Z., Richter, T. & Hansen, N. K. (1995). *XD User's Manual.* University of Berlin, Germany.

Le Campion, L., de Suzzoni-Dezard, S., Robic, N., Vandais, A., Varenne, P., Noel, J. P. & Quazzani, J. (1999). *J. Label. Compd Radiopharm.* **42**, 1203–1213.

Lee, K.-Y. & Coburn, M. D. (1988). US Patent 4,733,610.

Lee, K.-Y. & Gilardi, R. (1993). *Struct. Prop. Energet. Mater.* **296**, 237–242.

Murray, J. S., Lane, P. & Politzer, P. (1990). *J. Mol. Struct. (Theochem.)* **209**, 163–175.

Murray, J. S., Lane, P. & Politzer, P. (1995). *Mol. Phys.* **85**, 1–8.

Ritchie, J. P. (1989). *J. Org. Chem.* **54**, 3553–3560.

Sheldrick, G. M. (1996). *SADABS*. University of Göttingen, Germany.

Sheldrick, G. M. (1997). *SHELXTL*, Version 5.1. University of Göttingen, Germany.

Siemens (1996*a*). *SMART*5.054. Siemens Analytical X-ray Instruments Inc., Madison, Wisconsin, USA.

Siemens (1996*b*). *SAINT*. Siemens Analytical X-ray Instruments Inc., Madison, Wisconsin, USA.

Storm, C. B., Stine, J. R. & Kramer, J. F. (1990). *Chemistry and Physics of Energetic Materials*, edited by S. N. Bulusu, pp. 605–639. Dordrecht: Kluwer Academic Publishers.

Tsirelson, V. G., Ivanov, Yu., Zhurova, E. A., Zhurov, V. V. & Tanaka, K. (2000). *Acta Cryst.* B**56**, 197–203.

Tsirelson, V. G. & Ozerov, R. P. (1996). *Electron Density and Bonding in Crystals*, pp. 1–517. Bristol: Institute of Physics Publishing.

Volkov, A., Abramov, Yu., Coppens, P. & Gatti, C. (2000). *Acta Cryst.* A**56**, 332–339.